Influence of Branching on the Thermal Behavior of Poly(butylene isophthalate)

LARA FINELLI, NADIA LOTTI, ANDREA MUNARI

Dipartimento di Chimica Applicata e Scienza dei Materiali, University of Bologna, Viale Risorgimento 2, 40136 Bologna, Italy

Received 7 June 2001; Accepted 15 August 2001

ABSTRACT: The thermal behavior of linear and randomly branched poly(butylene isophthalate) samples was investigated by thermogravimetric analysis and differential scanning calorimetry. As to the thermal stability, it was found to be good and similar for all the samples. The thermal analysis carried out using DSC technique showed that the melting temperature of the polymers decreased with increasing branching unit content, although the glass-transition temperature was practically not affected by ramifications. The multiple endotherms typical of linear PBI were also observed in branched samples and were found to be influenced both by temperature and degree of branching. By applying the Hoffman–Weeks' method, the equilibrium melting temperatures of the polymers were obtained. The presence of a crystal–amorphous interphase was evidenced only for the branched samples and the interphase amount was found to increase as the branching unit content was increased. Isothermal melt crystallization kinetics was analyzed according to Avrami's treatment. The introduction of branching points was found to decrease the overall crystallization rate of poly(butylene isophthalate). Values of Avrami's exponent n close to 3 were obtained for all the samples, in agreement with a crystallization process originating from predetermined nuclei and characterized by three dimensional spherulitic growth. © 2002 Wiley Periodicals, Inc. J Appl Polym Sci 84: 2001–2010, 2002; DOI 10.1002/app.10517

Key words: poly(butylene isophthalate); branching; thermal properties; crystallization kinetics

INTRODUCTION

The incorporation of random branching units in linear polymers is known to affect drastically several of their properties both in solution and in bulk.[1] Therefore, in previous investigations some of us dealt with the synthesis and molecular and rheological characterization of linear and branched poly(butylene terephtalate) (PBT),[2–5] poly(ethylene terephthalate) (PET),[6] and poly(butylene isophthalate) (PBI).[7–9] Subsequently, given that it is well known that the presence of branches markedly changes the crystallization kinetics and melting behavior of linear polymers, the crystallization behavior of branched PBT was also investigated.[10]

To our knowledge, to date no studies have appeared on the thermal behavior of *branched* poly(butylene isophthalate); the only data available in the literature concern *linear* PBI.[11,12] Herein we report the results of a detailed investigation about the influence of long branches on the thermal behavior and isothermal crystallization kinetics of PBI, carried out to obtain information on

Correspondence to: A. Munari (andrea.munari@mail.ing.unibo.it).

Journal of Applied Polymer Science, Vol. 84, 2001–2010 (2002)

Table I Molecular and Thermal Characterization Data for Purified Linear and Branched PBI

Sample	X_t ($\times 10^2$)[a]	M_w ($\times 10^{-3}$)[b]	T_{id} (°C)	T_m (°C)[c]	ΔH_m (J/g)[c]	T_g (°C)[d]	ΔC_p (J/g°C)[d]
PBIL	0.0	57.4	389	140	54	26	0.344
1PBIB	0.7	83.7	390	135	53	25	0.340
2PBIB	1.5	NC	389	133	52	25	0.339
3PBIB	2.2	NC	390	131	53	26	0.342

NC, not calculated because the conversion was beyond the theoretical gel point, even though the sample shows to be completely soluble.[7]

[a] Mole fraction of trifunctional units.

[b] By total end-group content.

[c] First scan.

[d] Second scan on samples quenched from the melt.

the kinetic and thermodynamic parameters that control the crystalline growth of the polymer.

EXPERIMENTAL

Materials

Poly(butylene isophthalate) samples with different branching unit content (PBIB) were synthesized in bulk according to the well-known two-stage polycondensation procedure, as previously reported,[7] starting from dimethylisophthalate (DMI) and 1,4-butanediol (BD), using titanium tetrabutoxide [$Ti(OBu)_4$] as catalyst. The trifunctional monomer tris(hydroxy ethyl) isocianurate (THEIC) was added to the initial reaction mixture in small fractions (from 0.5 to 1.5 mol % with respect to DMI). The relatively high temperature adopted and the use of titanium tetrabutoxide led to generation of polymers with a random distribution of the trifunctional units and molecular weights.[13] The comonomeric units are, respectively,

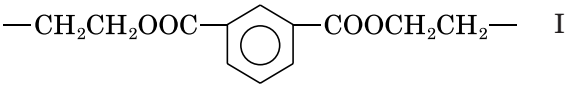

I

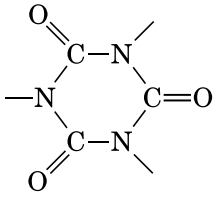

II

Linear poly(butylene isophthalate) (PBIL) was also synthesized under the same conditions to be taken as a comparison. Both PBIL and PBIB samples were purified according to the procedure previously described[7] and the molecular characterization data are reported in Table I.

Thermogravimetric Measurements

Thermogravimetric curves were obtained both in air and in nitrogen atmosphere using a Perkin–Elmer TGA7 apparatus (gas flow: 50 mL/min; Perkin Elmer Cetus Instruments, Norwalk, CT) at 10°C/min heating rate up to 900°C.

Calorimetric Measurements

Calorimetric measurements were carried out by means of a Perkin–Elmer DSC7 instrument (Perkin Elmer Cetus Instruments) equipped with a liquid subambient accessory and calibrated with high purity standards (indium and cyclohexane). The external block temperature control was set at −60°C. Weighed samples (~ 10 mg) were encapsulated in aluminum pans and heated to about 30°C above the fusion temperature at a rate of 20°C/min (first scan) and then rapidly quenched to −40°C. Finally, they were reheated from −40°C to the melting temperature at a heating rate of 20°C/min (second scan). The glass-transition temperature T_g was taken as the midpoint of the heat capacity increment Δc_p associated with the glass-to-rubber transition. The melting temperature (T_m) was determined as the peak value of the endothermal phenomenon in the DSC curve. The specific heat increment Δc_p, associated with the glass transition of the amorphous phase, was calculated from the vertical distance between the two extrapolated baselines at the glass-transition temperature. The heat of fusion of the crystal phase was calculated from the difference between the enthalpy associated with the melting

endotherm and the cold-crystallyzation exotherm whenever present. Repeated measurements on each sample showed excellent reproducibility.

To study the isothermal crystallization behavior of PBIL and PBIB samples, the measurements were carried out under a nitrogen atmosphere, by using a fresh specimen (~ 5 mg) for each run. The following standard procedure was employed: the samples were heated to about 30°C above the fusion temperature, then quickly cooled by liquid nitrogen to the crystallization temperature T_c. The T_c range was chosen to avoid crystallization during the cooling step and to obtain crystallization times no longer than 60 min. The heat flow evolving during the isothermal crystallization was recorded as a function of time and the completion of the crystallization process was detected by the leveling of the DSC trace. For a better definition of the starting time, for each isothermal scan, blank runs were also performed with the same sample, at a temperature above the melting point where no phase change occurred.[10] The blank runs were subtracted from the isothermal crystallization scan and the start of the process was taken as the intersection of the extrapolated baseline and the resulting exothermal curve. The isothermally crystallized samples were then heated directly from T_c to melting at 10°C/min.

To obtain samples characterized by different crystal/amorphous ratios, the samples were partially melted in DSC by heating to various temperatures in the melting range, quickly cooled below the glass-transition temperature, and reheated at 20°C/min.

RESULTS AND DISCUSSION

The TGA measurements carried out in air or under nitrogen atmosphere led to similar results: for all the samples synthesized the thermal decomposition takes place practically in one step and is 100%. The initial decomposition temperature (T_{id}) for linear as well as branched samples in air are reported in Table I. All the branched samples showed good thermal stability and relatively high temperature of decomposition with only slight differences with respect to PBIL.

It is well established that the melting behavior of a polymer is affected by its previous thermal history. To provide the same thermal treatment to all samples investigated, specimens were annealed at 90°C for 8 days in an oven under vacuum. The calorimetric results, reported in Table I, indicate that the introduction of small amounts of branching units leads to a reduction of the melting temperature of poly(butylene isophthalate).

As far as the enthalpy of fusion is concerned, an estimate after normalization for the linear butylene isophthalate units content leads in all cases to a value of 54 J/g, which corresponds to 43% of crystallinity, assuming 125 J/g as the heat of fusion of perfectly crystalline PBI.[12] Therefore, the random incorporation of small amounts of noncrystallizable branching units into the PBI backbone, even if it leads to a depression of the melting temperature, does not influence the total crystallinity degree of PBI, which crystallizes in the copolymer in the same percentage as that in the pure state. Analogous results were found in some investigations of the effect of long branches on PBT.[10]

A partially crystalline material is expected to exhibit different glass-transition behavior than that of completely amorphous material. Although some conflicting results are reported in the literature,[14] crystallinity usually acts like crosslinking and raises T_g through its restrictive effect on segmental motion of amorphous polymer chains. To study the influence of chemical structure on the glass transition of random copolymers, the phenomenon should be examined in the total absence of crystallinity. Rapid cooling (quenching) from the melt is the method commonly used to prevent crystallization and to obtain polymers in a completely amorphous condition.

By adopting the experimental procedure described above, completely amorphous PBIL and PBIB samples were obtained, as evidenced by the corresponding DSC curves, characterized by an intense endothermal baseline deviation associated with the glass transition. The values of T_g and of the specific heat increment Δc_p associated with the glass transition are collected in Table I; as can be seen, both T_g and Δc_p do not change with composition, indicating no effect of branching on the glass-transition phenomenon in the samples under investigation.

Melting Behavior of Isothermally Crystallized Samples

Figure 1 shows the DSC heating curves of linear and branched PBI after isothermal crystallization from the melt. The isothermal crystallization and the melting behavior of 3PBIB could not be investigated because of the too low rate of crystalliza-

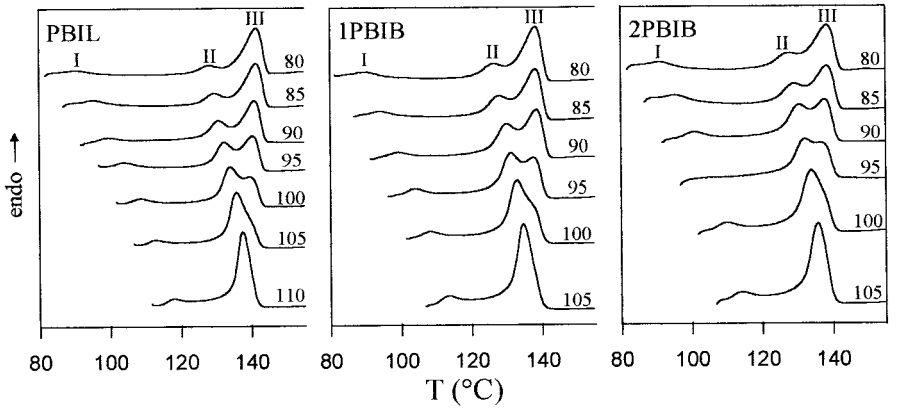

Figure 1 DSC melting endotherms after isothermal crystallization at the indicated T_c's (heating rate: 10°C/min).

tion. As can be seen, all the samples display multiple endotherms, whose peaks have been labeled with Roman numerals (I to III) in order of increasing temperature. It is well known that a lot of semicrystalline polymers as well as their copolymers show multiple endothermic peaks.[10,15–17] There has been much discussion in the literature as to the possible origin of the phenomenon: multiple endotherms can be attributed to the presence of two or more groups of crystals with different morphologies or lamellar thickness[15] or they can be ascribed to a recrystallization process occurring during the DSC scan.[10,16] In addition, both processes could operate at different undercooling degrees.[17] The multiple endotherm behavior is typical of many polyesters, for the best-studied of which the phenomenon has often been ascribed to a reorganization process taking place during the DSC scan.[10,16] In particular, endotherm I, which appears as a small peak at about 10°C above T_c, is usually attributed to the melting of crystals formed during a secondary crystallization process.[18] Endotherm II is ascribed to the fusion of the crystal population grown during the isothermal period at T_c. It exhibits a strong dependency on crystallization temperature, in terms of both peak position and area, that is, the endotherm appears at higher temperatures and its area progressively increases as the T_c increases. Such an increase suggests that thicker crystalline lamellae develop with increasing T_c. In contrast to endotherms I and II, the location of the highest temperature melting endotherm (III), whose intensity decreases with increasing T_c, shows no dependency on the crystallization temperature.

To investigate deeply the nature of these multiple endotherms, the effect of the scanning rate on the melting behavior of linear and branched PBI samples was analyzed. It can be observed (see Fig. 2) that (1) the endotherm III moves to higher temperatures as the heating rate decreases and (2) the ratio between the area of the second melting peak and the third one increases as the heating rate is increased, confirming that the multiple melting in linear and branched PBI results from a mechanism based on melting and recrystallization of less-perfect crystallites into thicker crystals, followed by a final melting process at a higher temperature.

Experimental melting temperatures of the copolymers crystallized at different T_c's are commonly used to obtain information on the equilibrium melting temperature T_m° by means the Hoffman–Weeks' relationship[19]:

$$T_m = T_m^\circ(1 - 1/\gamma) + T_c/\gamma \qquad (1)$$

where γ is a factor that depends on the lamellar thickness. More precisely, $\gamma = l/l^*$, where l and l^* are the thickness of the grown crystallite and of the critical crystalline nucleus, respectively.[20] It has to be pointed out that eq. (1) correctly represents experimental data only when γ is constant and the slope of the curve in a plot T_m versus T_c plot is approximately equal to 0.5.[20]

Although the concept of infinite lamellar thickness is appropriate only for homopolymers,[20] the Hoffman–Weeks' treatment is frequently applied to copolymers, too,[20–23] to obtain the driving force for crystallization (i.e., the degree of undercooling $\Delta T = T_m^\circ - T_c$). The extrapolated T_m° data can be also used to evaluate the melting point depression induced by the presence of the second noncrystallizable component.[24]

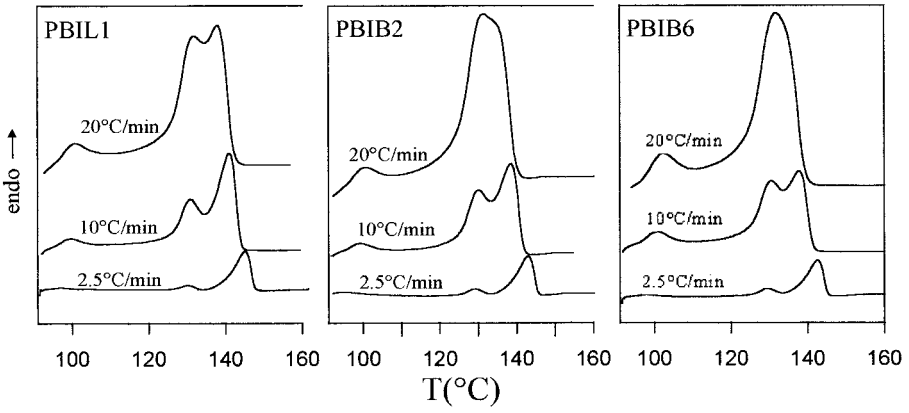

Figure 2 DSC melting endotherms scanned at the indicated heating rate after isothermal crystallization at 90°C. The curves are not corrected for the changes in the instrumental signal with heating rate.

As an example, the T_m versus T_c plot for the linear PBI sample is shown in Figure 3: endotherm II is clearly related to the original main crystal population and its location reflects the higher perfection of the crystals grown at higher temperatures. The marked deviation from linearity found at low T_c values is symptomatic of the fast reorganization process involving imperfect crystallites during the DSC heating. The melting endotherm III is observed at a rather constant temperature, characteristic of the material partially recrystallized into a more stable form on heating. As a matter of fact, with increasing T_c, the originally grown crystals improve their degree of perfection up to a point where no further recrystallization can occur during the DSC run and endotherm III disappears. In Figure 3 the linear extrapolation of the experimental data up to the $T_m = T_c$ line is also drawn, and a T_m° value of 156°C was obtained. This result appears to be in perfect agreement with the datum previously found by some of us investigating the as-prepared linear PBI.[12] As far as branched PBI are concerned, the extrapolated values of T_m° were found to be 154 and 152 for 1PBIB and 2PBIB, respectively, indicating that the equilibrium melting temperature slightly decreases with increasing branching unit content. The observed decrease of the melting temperature can be explained assuming that the branching points act as defects in the crystalline structure, producing, as a consequence, a reduction in the lamellar thickness.[25,26] Similar results were found in investigating the thermal behavior of the samples not subjected to isothermal treatments (see above) and confirm the exclusion of branching units from the crystalline lattice of PBI.

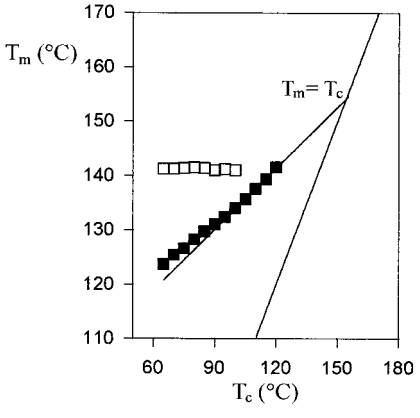

Figure 3 Peak temperature of middle (■) and high (□) temperature endotherms as a function of T_c for PBIL and linear extrapolation according to the Hoffman–Weeks' treatment.

Thermodynamic Parameters

To evaluate the heat of fusion of completely crystalline samples, the relationship between the specific heat increment at T_g and the heat of fusion of samples with different crystal/amorphous ratios was examined. The experimental enthalpy of fusion was normalized for the linear butylene isophthalate weight fraction. The ΔH_m values obtained are plotted as a function of Δc_p in Figure 4. The specific heat increment is seen to decrease regularly as the melting enthalpy increases and the experimental data are well represented by a straight line. A two-phase model was applied to

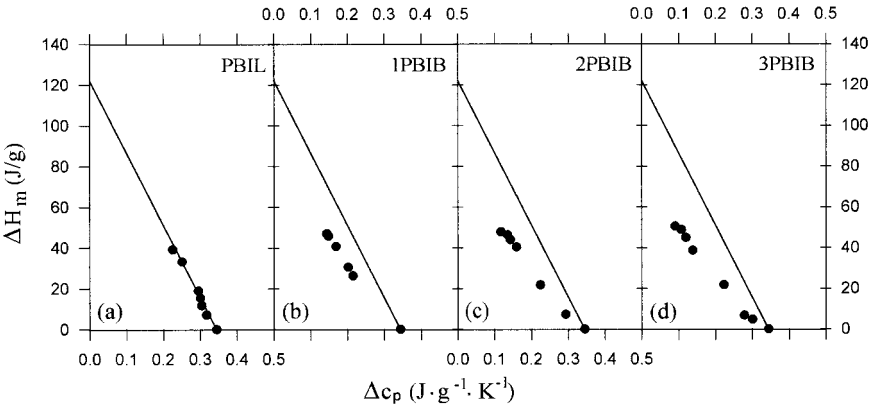

Figure 4 Heat of fusion ΔH_m (normalized for the crystallizable component weight fraction) as a function of the specific heat increment Δc_p at T_g. Solid lines: $\Delta H_m - \Delta c_p$ lines calculated on the basis of a two-phase model.

the copolymers under investigation and the $\Delta H_m - \Delta c_p$ dependency (solid line), calculated on the basis of this model and the additivity of the specific heat increments, is reported in Figure 4 for all the samples, according to the equation:

$$\Delta c_p = w_A \Delta c_{p,A} + w_B(1 - \Delta H_m/\Delta H_m^\circ)\Delta c_{p,B} \quad (2)$$

where Δc_p, $\Delta c_{p,A}$, and $\Delta c_{p,B}$ are the specific heat increments of copolymer and homopolymers A and B, respectively; w_A and w_B are the weight fractions of A and B units; ΔH_m is the normalized melting enthalpy associated with the fusion of the crystallizable units; and ΔH_m° is the equilibrium melting enthalpy of the crystallizable component. It is clear from Figure 4 that the two-phase prediction is not satisfied, given that the experimental specific heat increments of semicrystalline samples are considerably lower than expected for the full mobilization of the noncrystalline fraction. In addition, Figure 4 clearly shows that the deviation from the two-phase model increases with increasing crystallinity and is greater for the sample with higher content of noncrystallizable component (branching units). This is a consequence of the fact that often in polymers there is not a sharp separation between the crystalline and the amorphous phases[18,27,28] and constraints imposed by the crystallites are expected on noncrystallizable units linked to crystal surfaces. Consequently, three distinguishable phases can coexist in a semicrystalline copolymer: (1) a crystalline phase, attributed to the crystallizable component; (2) a "normal" amorphous phase; and (3) an interphase (or rigid amorphous phase) occurring in the vicinity of the crystallites. An interphase is defined as that portion of noncrystalline material that does not mobilize at the glass-transition temperature and therefore does not contribute to the observed specific heat increment.

To determine the interphase content as a function of copolymer composition, the weight fractions of the crystalline phase (w_c), amorphous phase (w_a), and interphase (w_i) were calculated according to the following relationships:

$$w_c = (\Delta H_m w_{BI})/\Delta H_m^\circ \quad (3)$$

$$w_a = \Delta c_p/\Delta c_p^a \quad (4)$$

$$w_i = 1 - w_c - w_a \quad (5)$$

where Δc_p and Δc_p^a correspond to the experimental specific heat increments of the semicrystalline and fully amorphous copolymer, respectively, and w_{BI} is the weight fraction of butylene isophthalate units. The variation of the interphase weight fraction as a function of the copolymer composition can be analyzed for a given crystallinity degree of the crystallizable component $x_c = \Delta H_m/\Delta H_m^\circ$. The results are shown in Figure 5 for x_c values of 0.20 and 0.30. The crystallinity, as expected, decreases with increasing the percentage of the noncrystallizable component, but the amorphous content also shows a reduction. As a matter of fact, there is an increase in the results of the calculated interphase weight fraction. As already mentioned, the noncrystallizable comonomer hinders the crystallization process, leading to small and

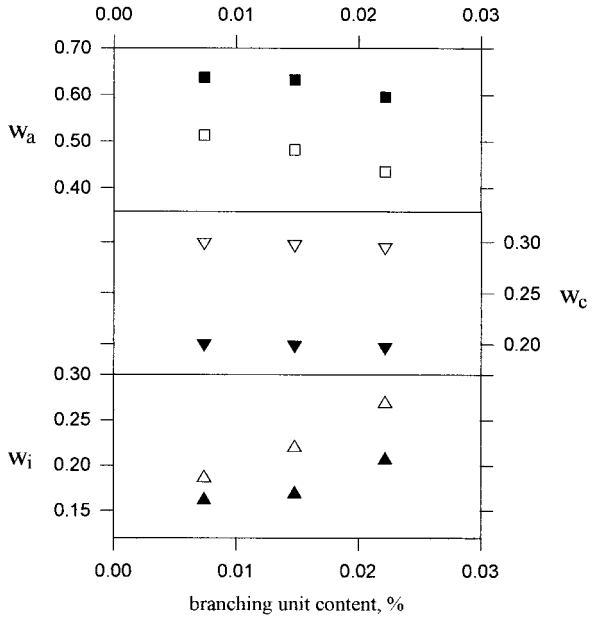

Figure 5 Weight fractions of amorphous phase (w_a), crystalline phase (w_c), and interphase (w_i) as a function of branching unit content (filled symbols: $x_c = 0.20$, open symbols: $x_c = 0.30$).

imperfect crystallites. The crystalline phase turns out to be highly dispersed, and the increase in crystal surface results in extensive constraints on the amorphous phase.

Crystallization Kinetics

The analysis of the isothermal crystallization kinetics can be carried out on the basis of the Avrami equation[29]:

$$X_t = 1 - \exp[-k_n(t - t_{\text{start}})^n] \quad (6)$$

where X_t is the fraction of polymer crystallized at time t; k_n is the overall kinetic constant; t is the time of the isothermal step measured from the achievement of the temperature control; t_{start} is the initial time of the crystallization process, as described in the Experimental section; and n the Avrami exponent, which is correlated with the nucleation mechanism and the morphology of the growing crystallites. X_t can be calculated as the ratio between the area of the exothermic peak at time t and the total measured area of crystallization. Equation (6) is usually applied to the experimental data in the linearized form, by plotting $\ln[-\ln(1 - X_t)]$ as a function of $\ln(t - t_{\text{start}})$ and the values of n and k_n can be acquired from the slope and the intercept, respectively. The value of the kinetic constant k_n is also frequently obtained through the following relation:

$$k_n = \ln 2/t_{1/2}^n \quad (7)$$

where $t_{1/2}$ is the crystallization half-time, defined as the time required to reach $X_t = 0.5$.

In Figure 6, typical linearized Avrami plots for PBIL, 2PBIB, and 3PBIB samples are shown for selected sets of crystallization temperatures. The observed deviation from the linear behavior at long times is attributed to secondary crystallization phenomena.[29]

The crystallization half-time $t_{1/2}$, the parameter n, and the kinetic constants k_n are collected in Table II.

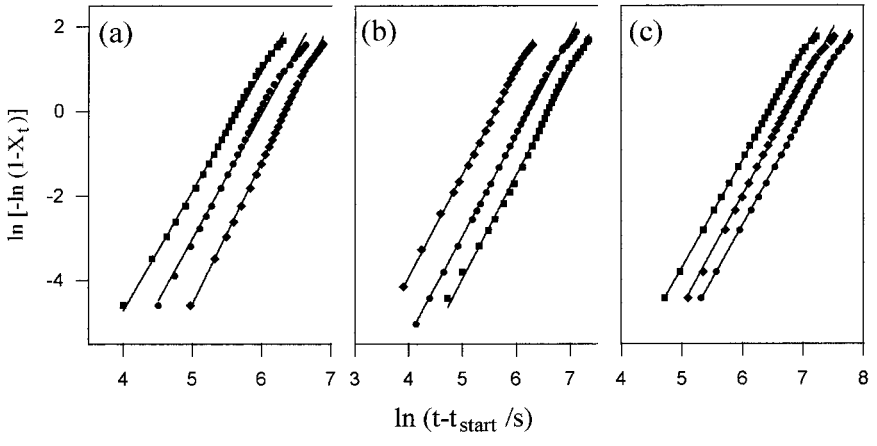

Figure 6 Avrami plots for: (a) PBIL at T_c: (■) 90°C, (●) 110°C, (◆) 115°C; (b) 1PBIB at T_c: (●) 70°C, (◆) 100°C, (■) 115°C; (c) 2PBIB at T_c: (●) 75°C, (■) 95°C, (◆) 105°C.

Table II Kinetic Parameters for the Isothermal Crystallization of Linear and Branched PBI

Sample	T_c (°C)	$t_{1/2}$ (min)	n	k_n (s^{-n})	E_a (kcal/mol)
PBIL	60	20.9	3.0	1.1×10^{-9}	59
	65	12.6	2.8	7.2×10^{-9}	
	70	8.1	2.8	3.8×10^{-8}	
	75	5.5	2.8	9.4×10^{-8}	
	80	4.5	2.8	2.5×10^{-7}	
	85	3.5	2.7	6.3×10^{-7}	
	90	3.6	2.7	1.3×10^{-6}	
	95	3.9	2.8	3.4×10^{-7}	
	100	4.5	2.9	1.4×10^{-7}	
	105	5.7	3.1	2.6×10^{-8}	
	110	7.6	3.2	5.1×10^{-9}	
	115	10.3	3.5	4.5×10^{-10}	
	120	16.8	3.5	1.1×10^{-11}	
1PBIB	60	25.6	2.8	4.3×10^{-10}	63
	65	13.3	2.8	5.6×10^{-9}	
	70	8.9	2.8	1.7×10^{-8}	
	75	6.5	2.7	7.7×10^{-8}	
	80	5.1	2.7	1.9×10^{-7}	
	85	4.4	2.7	4.0×10^{-7}	
	90	3.9	2.7	4.9×10^{-7}	
	95	4.3	2.8	3.2×10^{-7}	
	100	4.8	3.0	1.4×10^{-7}	
	105	5.8	3.1	8.7×10^{-9}	
	110	8.2	3.1	2.2×10^{-9}	
	115	14.0	3.2	1.4×10^{-10}	
	120	30.3	3.6	3.0×10^{-13}	
2PBIB	70	29.7	3.3	1.5×10^{-11}	139
	72.5	23.9	3.2	7.9×10^{-11}	
	75	21.2	3.0	4.5×10^{-10}	
	77.5	17.6	2.9	2.3×10^{-9}	
	80	13.7	2.9	3.6×10^{-9}	
	85	13.1	2.9	1.6×10^{-8}	
	90	12.0	2.8	1.3×10^{-8}	
	95	12.6	2.9	5.0×10^{-9}	
	100	13.8	3.1	1.2×10^{-9}	
	105	15.7	3.1	4.8×10^{-10}	
	110	21.8	3.3	7.7×10^{-11}	
	115	30.1	3.3	2.3×10^{-11}	

It is worth remembering that the crystallization kinetics of the as-prepared PBI was investigated by some of us.[12] From a comparison of our data with those previously reported, it was found that the purified sample crystallizes much faster than the as-prepared one. This relevant discrepancy may be ascribed to the large amount of cyclic oligomers in the as-prepared PBI.[7] As a matter of fact, these cyclic oligomers represent defects that have to be rejected from the crystalline phase.

To evaluate the effect of composition on crystallization rate, the half-crystallization time $t_{1/2}$ was plotted as a function of undercooling degree ($\Delta T = T^{\circ}_m - T_c$), shown in Figure 7 for the samples under investigation. An increase in $t_{1/2}$ is observed as the content of branching units is increased. Taking into account that the crystallization of a single component in copolymers involves the segregation of the noncrystallizable units, the observed decrease of the crystallization rate with increasing branching unit content is probably related to the branching points, which act as obstacles in the regular packing of polymer chains. In particular, as shown in Figure 7, the experimental results show a minimum in the $t_{1/2}$– T_c curve, that is, a maximum in the corresponding k_n– T_c dependency. It is worth remembering that the crystallization kinetics is controlled by a nucle-

ation process or by polymer chain diffusion in the melt, depending on the crystallization temperature. At low T_c (high undercooling) the determining step is represented by diffusion of the polymer segments, whereas at high T_c (low undercooling) the determining step is the nucleation process, given that its rate is very low. As a consequence, the overall crystallization rate goes through a maximum (minimum in $t_{1/2}$). Therefore, the results shown in Figure 7 indicate that all the samples investigated are characterized by a low nucleation rate, which allows high undercooling to be reached without crystallization taking place during the cooling step.

To get some idea of the activation energy (E_a) for the crystallization process, plots of ln k_n versus $1/T$ were derived for each sample, considering exclusively the data in the temperature range where the crystallization process is controlled by chain diffusion. In all cases, the plots exhibit a good linearity, as illustrated in Figure 8. The activation energies, estimated from the slope ln k_n versus $1/T$ plots, are collected in Table II and appear to be affected by composition, increasing as the content of branching units is increased. This result can be considered a further evidence of the fact that branching points hinder the crystallization of PBI and therefore act as defects in the crystalline structure of the linear polymer.

The Avrami exponent n is very close to 3 for all the polymers investigated (see Table II), indicating that the crystallization process originates from predetermined nuclei and is characterized by three-dimensional spherulitic growth. Indeed, some optical microscopy observations that we have carried out have revealed a spherulitic morphology in isothermally crystallized linear and branched PBI.

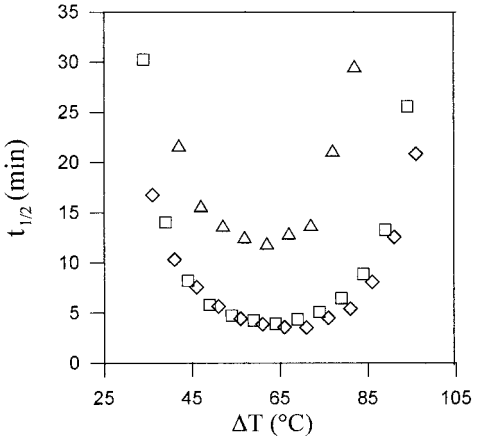

Figure 7 Crystallization half-time ($t_{1/2}$) as a function of ΔT for: (◇) PBIL; (□) 1PBIB; (△) 2PBIB.

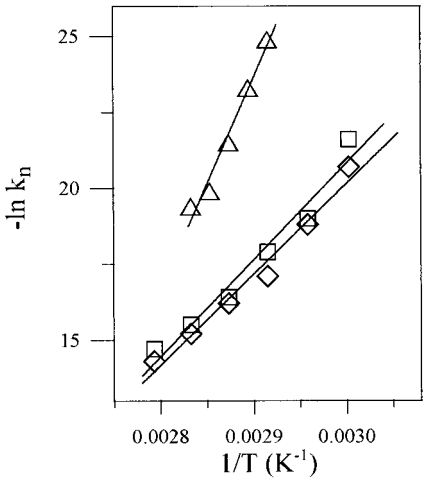

Figure 8 Arrhenius plots for: (◇) PBIL; (□) 1PBIB; (△) 2PBIB. Solid lines: fitting curves according to the Arrhenius-type equation.

REFERENCES

1. Roovers, J. in Encyclopedia of Polymer Science and Technology, 2nd ed.; Wiley: New York, 1985; Vol. 2.
2. Pilati, F.; Munari, A.; Manaresi, P. J Mater Chem 1982, 7, 649.
3. Pilati, F.; Munari, A.; Manaresi, P. J Mater Chem 1982, 7, 661.
4. Munari, A.; Pilati, F.; Pezzin, G. Rheol Acta 1984, 23, 14.
5. Munari, A.; Pilati, F.; Pezzin, G. Rheol Acta 1985, 24, 534.
6. Manaresi, P.; Parrini, P.; Semeghini De Fornasari, G. L. E. Polymer 1976, 17, 595.
7. Pilati, F.; Munari, A.; Manaresi, P.; Milani, G.; Bonora, V. Eur Polym J 1987, 23, 265.
8. Munari, A.; Pilati, F.; Pezzin, G. Rheol Acta 1988, 27, 145.
9. Munari, A.; Pilati, F.; Pezzin, G. Rheol Acta 1990, 29, 469.
10. Righetti, M. C.; Munari, A. Macromol Chem Phys 1997, 198, 363.
11. Righetti, M. C.; Pizzoli M.; Munari, A. Macromol Chem Phys 1994, 195, 2039.
12. Righetti, M. C.; Pizzoli M.; Lotti, N.; Munari, A. Macromol Chem Phys 1998, 199, 2063.
13. Pilati, F. in Comprehensive Polymer Science; Allen, G.; Bevington, J. C., Eds.; Pergamon Press: Oxford, 1989; Vol. 5, Chapter 17.
14. Boyer, R. F. Rubber Chem Technol 1963, 36, 1303.
15. Basset, D. C.; Olley, R. H.; Al Raheil, I. A. M. Polymer 1988, 29, 1745.

16. Holdsworth, P. J.; Turner-Jones, A. Polymer 1971, 12, 195.
17. Chung, J. S.; Cebe, P. Polymer 1992, 33, 2312.
18. Wunderlich, B. Macromolecular Physics, Vols. 2 and 3; Academic Press: New York, 1976, 1980.
19. Hoffman, J. D.; Weeks, J. J. J Res Natl Bur Stand (US) 1962, 66A, 13.
20. Alamo, R. G.; Viers, B. D.; Mandelkern, L. Macromolecules 1995, 28, 3205.
21. Wu, S. S.; Kalika, D. S.; Lamonte, R. R.; Makhija, S. J Macromol Sci Phys 1996, B35, 157.
22. Orler, E. B.; Calhoun, B. H.; Moore, R. B. Macromolecules 1996, 29, 5965.
23. Lee, S. W.; Lee, B.; Ree, M. Macromol Chem Phys 2000, 201, 453.
24. Godbeck-Wood, G. Polymer 1992, 33, 778.
25. Manaresi, P.; Munari, A.; Pilati, F.; Alfonso, G. C.; Russo, S.; Sartirana, M. L. Polymer 1986, 27, 955.
26. Lopez, L. C.; Wilkes, G. L.; Geibel, J. F. Polymer 1986, 27, 955.
27. Manderkern, L. in Comprehensive Polymer Science, Vol. 2; Allen, G.; Bevington, J. C., Eds.; Pergamon Press: Oxford, 1988.
28. Cheng, S. Z. D.; Wunderlich, B. Macromolecules 1988, 21, 789.
29. Avrami, M. J Chem Phys 1941, 9, 177.